CALCULATION OF THE VELOCITY PROFILE IN THE FLOW OF A NONLINEAR VISCOELASTIC FLUID IN A CHANNEL WITH HELICAL KNURLING

Yu. G. Nazmeev and I. A. Konakhina

UDC 678:532.135

The formulation, methods, and results of a solution of the problem of flow of a nonlinear viscoelastic fluid in a channel with helical knurling are presented.

Research in the field of the intensification of heat-transfer processes has shown that one of the most efficient and constructively convenient to implement methods of enhancing convective heat and mass transfer is to use artificial turbulizers in the boundary region of flow. The well-known published experimental data on intensification using annular or helical internal ribbing in pipes and using spiral coil inserts [1-3] permit the conclusion that they are fairly efficient. Helical knurling on the surface of a pipe (Fig. 1) can also increase the intensity of heat-transfer processes. This is especially important for flows of high-viscosity media, characterized by low Reynolds and Nusselt numbers.

In the solution of problems associated with the investigation of convective heat and mass transfer in channels, the hydrodynamic part of the problem is particularly complicated. It therefore seems important to isolate that part, which is associated with determining the distribution of the velocity vector in the channel.

Let us consider the problem of determining the velocity profile that is formed in the laminar flow of a nonlinear viscoelastic fluid in a channel with helical knurling. A model of the differential type is used to describe the rheological properties of the fluid. The stress tensor at time t is represented by a nonlinear symmetric tensor functional of the history of deformation and can be expanded in a Taylor series in the vicinity of $t = 0$ with respect to N-th order White–Metzner kinematic tensors B_N [4],

$$B_{N+1}=\frac{d}{dt}(B_N)-(B_N\cdot\nabla\bar{V}^t)-(\nabla\bar{V}\cdot B_N),$$

$$B_1=2D,$$

where $D = (\nabla\bar{V} + \nabla V^t)/2$ is the deformation-rate tensor.

In general, the system of equations describing this problem and including the equations of motion and continuity has the form

$$(\bar{V}\cdot\operatorname{grad}\bar{V})=-\frac{1}{\rho}\operatorname{grad}P+\frac{1}{\rho}\operatorname{div}(T^0), \tag{1}$$

$$\operatorname{div}(\bar{V})=0, \tag{2}$$

$$\bar{V}|_b=0, \tag{3}$$

where T^0 is the stress tensor deviator.

All of the boundaries of the channel under consideration can be represented by a family of helical surfaces, and a helical channel, as shown in [5], possesses one-parameter helical group symmetry, regardless of the shape of its cross section. Because of this, the velocity field being sought can be assumed to be independent of the coordinate directed along the channel axis (q^3).

We introduce nonorthogonal helical coordinates [6], related to cylindrical coordinates by the equations

Kazan' Branch of the Moscow Power Institute. Translated from Inzhenerno-Fizicheskii Zhurnal, Vol. 62, No. 3, pp. 373-379, March, 1992. Original article submitted June 24, 1991.

 1062-0125/92/6203-0270 $12.50

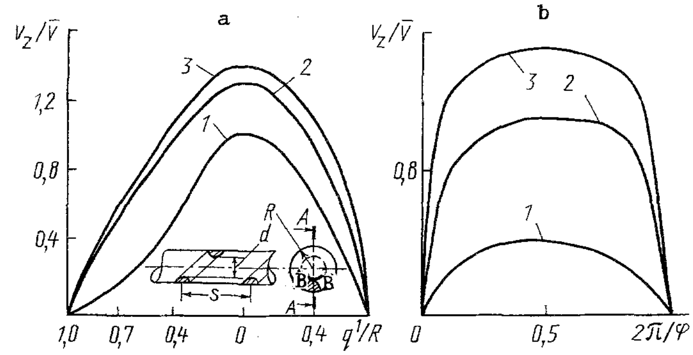

Fig. 1. Calculated profiles of the axial component of the velocity vector: a) radial cross section A–A; b) annular cross section B–B; 1) S/D = 0.72; 2) 1.79; 3) 2.86.

$$q^1 = r,\ q^2 = \varphi - kz,\ q^3 = z. \tag{4}$$

The contravariant helical components by the velocity vector will then be related to the cylindrical components by the equations

$$V^1 = V_r,\ V^2 = V_\varphi - kV_z,\ V^3 = V_z. \tag{5}$$

The stress tensor for the investigated fluid will have the form

$$\sigma = -PI + \varphi_1(I_2)B_1 + \varphi_2(I_2)B_2,$$

where $I_2 = \mathrm{tr}(B_1^2)$.

We shall assume that the flow under consideration is viscosimetric, in the subclass of helical flows [4]. The dependence of the material functions φ_1 and φ_2 on I_3 can then be neglected.

We approximate the behavior of the functions φ_1 and φ_2 by power-law functions,

$$\varphi_i(I_2) = K_i(I_2)^{n_i},\ i = \overline{1,\ 2}.$$

Statement of the Problem in the Galerkin Approximation. The generalized solution of the initial system of hydrodynamic equations (1)-(2) with the boundary condition (3) must satisfy the integral equation

$$\iiint_L \{(\rho(V\cdot\mathrm{grad}\,V)\cdot\bar{h}) - (\mathrm{div}\,(T^0)\cdot\bar{h}) + (\mathrm{grad}\,P\cdot\bar{h})\}\,dL = 0,$$

where $\bar{h}$ is an arbitrary element of the space of solenoidal vector functions $H_2^1(\Omega)$. The boundary condition (3) is then satisfied for $\bar{h}$, as well, i.e., $\bar{h}|_b = 0$. For a sequence of basis functions $h^{(1)}$, $h^{(2)}$, ..., $h^{(n)}$ belonging to the space $H_2^1(\Omega)$, the following must be satisfied:

$$\iint_\Omega \{\varphi_1 B_1(V^{(n)}): D(h^{(k)}) + \varphi_2 B_2(V^{(n)}): D(h^{(k)}) + (\rho(V^{(n)}\,\mathrm{grad}\,V^{(n)}) + \mathrm{grad}\,P)\,h^{(k)}\}\,d\Omega = 0. \tag{6}$$

By analogy with [7], the system (6), representing a functional operator L_0 defined by the expression $(L_0V,\ h) = 0$, can be expressed in terms of two operators L_1 and L_2 for which the relationships $(L_1V,\ h) = 0$ and $(L_2V,\ h) = 0$ are satisfied. This enables us to take only $\partial P/\partial q^3$ into account in the system (6), which was proven in [7].

We thus have

$$\begin{aligned}(L_1V,\ h) = \iint_\Omega \Big\{ \varphi_1 \Big[&\frac{\partial V^{1(n)}}{\partial q^1}\frac{\partial h^{1(k)}}{\partial q^1} + \left(\frac{\partial V^{2(n)}}{\partial q^1} + \frac{A}{(q^1)^2}\frac{\partial V^{1(n)}}{\partial q^2}\right)\frac{\partial h^{1(k)}}{\partial q^2} + \\ &+ \left(\frac{2}{q^1}\frac{\partial}{\partial q^2}(V^{2(n)} + kV^{3(n)}) - \frac{2}{(q^1)^2}V^{1(n)}\right)h^{1(k)} + \Big((q^1)^2\frac{\partial}{\partial q^1}(V^{2(n)} + \\ &+ kV^{3(n)}) + \frac{\partial V^{1(n)}}{\partial q^2}\Big)\frac{\partial h^{2(k)}}{\partial q^1} + \left((A+1)\frac{\partial V^{2(n)}}{\partial q^2} + Ak\frac{\partial V^{3(n)}}{\partial q^2} + \frac{2}{q^1}V^{1(n)}\right)\frac{\partial h^{2(k)}}{\partial q^2} + \\ + 2k^2\varphi_2\Big]\Big[q^1\left(\frac{\partial V^{3(n)}}{\partial q^1}\right)^2 + \frac{A}{q^1}\left(\frac{\partial V^{3(n)}}{\partial q^2}\right)^2\Big]&h^{1(k)} + \rho(V^{(n)}\,\mathrm{grad}\,V^{(n)})_1 h^{1(k)} + \rho(V^{(n)}\,\mathrm{grad}\,V^{(n)})_2 h^{2(k)}\Big\}\,d\Omega = 0,\end{aligned} \tag{7}$$

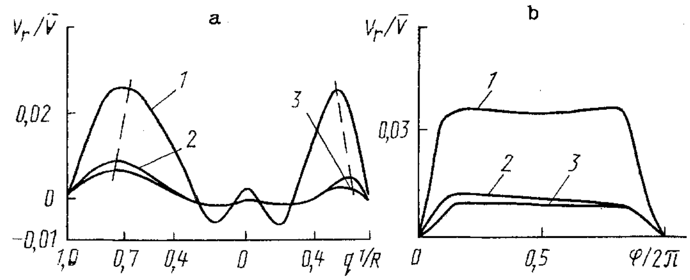

Fig. 2. Calculated profiles of the radial component of the velocity vector (notation same as in Fig. 1).

$$(L_1V,\ h) = \iint_\Omega \left\{ \varphi_1 \left[\left[A \frac{\partial V^{3(n)}}{\partial q^1} + k(q^1)^2 \frac{\partial V^{2(n)}}{\partial q^1} \right] \frac{\partial h^{3(k)}}{\partial q^1} + \left[\frac{A^2}{(q^1)^2} \frac{\partial V^{3(n)}}{\partial q^2} + AK \frac{\partial V^{2(n)}}{\partial q^2} + \frac{2k}{q^1} V^{1(n)} \right] \frac{\partial h^{3(k)}}{\partial q^2} \right] + \frac{\partial P}{\partial q^3} h^{3(k)} \right\} d\Omega = 0. \tag{8}$$

With allowance for the helical symmetry of flow demonstrated in [5], one can show that $\partial P/\partial q^3 = C = \mathrm{const}$. We determine $\partial P/\partial q^3$ using Eq. (8):

$$\frac{\partial P}{\partial q^3} = -\frac{1}{Q} \iint_\Omega \left\{ \varphi_1 \left[\left(A \frac{\partial V^3}{\partial q^1} + k(q^1)^2 \frac{\partial V^2}{\partial q^1} \right) \frac{\partial V^3}{\partial q^1} + \left(\frac{A}{(q^1)^2} \frac{\partial V^3}{\partial q^2} + Ak \frac{\partial V^2}{\partial q^2} + \frac{2k}{q^1} V^1 \right) \frac{\partial V^3}{\partial q^2} \right] \right\} d\Omega.$$

Statement of the Problem in the Vorticity–Stream Function Form. We introduce new functions into the system (1)-(3) under consideration: the stream function ψ, related to the components V^1 and V^2 by the equations

$$\frac{1}{q^1} \frac{\partial \psi}{\partial q^2} = V^1, \quad -\frac{1}{q^1} \frac{\partial \psi}{\partial q^1} = V^2,$$

and a third contravariant component ω^3 of the vorticity. The initial system of differential equations then takes the form

$$2\rho q^1 [\mathrm{curl}(V \cdot \mathrm{grad}\, V)]_3 = \frac{\partial^2 T^0_{21}}{(\partial q^1)^2} + \frac{\partial^2}{\partial q^1 \partial q^2} \left[\frac{A}{(q^1)^2} T^0_{21} - kT^0_{23} - T^0_{11} \right] - \frac{\partial^2}{(\partial q^2)^2} \left[\frac{A}{(q^1)^2} T^0_{12} - kT^0_{13} \right] + \frac{\partial}{\partial q^1} \left[\frac{T^0_{11}}{q^1} - \frac{T^0_{22}}{(q^1)^3} - \frac{T^0_{21}}{q^1} \right] - \frac{\partial}{\partial q^2} \left[\frac{T^0_{11}}{q^1} - \frac{T^0_{22}}{(q^1)^3} \right]; \tag{9}$$

differential equations for the components of the deviator of the stress tensor, T^0_{ij} ($i = \overline{1, 3}$; $j = \overline{1, 3}$), are given in the Appendix;

$$\omega^3 = \frac{1}{2q^1} \left[\frac{\partial}{\partial q^1} \left[(q^1)^2 \left(kV^3 - \frac{1}{q^1} \frac{\partial \psi}{\partial q^1} \right) \right] - \frac{1}{q^1} \frac{\partial^2 \psi}{(\partial q^2)^2} \right]; \tag{10}$$

$$\frac{\partial P}{\partial q^3} = \frac{1}{q^1} \frac{\partial}{\partial q^1} \left[q^1 \varphi_1 \left(A \frac{\partial V^3}{\partial q^1} - kq^1 \frac{\partial}{\partial q^1} \left(\frac{1}{q^1} \frac{\partial \psi}{\partial q^1} \right) \right) \right] + \frac{\partial}{\partial q^2} \left[\varphi_1 \left(\frac{A^2}{(q^1)^2} \frac{\partial V^3}{\partial q^2} - \frac{Ak}{q^1} \frac{\partial^2 \psi}{\partial q^1 \partial q^2} + \frac{2k}{(q^1)^2} \frac{\partial \psi}{\partial q^2} \right) \right] \tag{11}$$

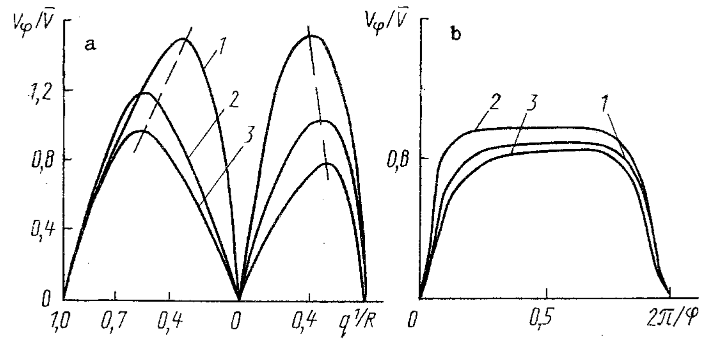

Fig. 3. Calculated profiles of the centrifugal component of the velocity vector (notation as in Fig. 1).

with the boundary conditions $\psi|_b = 0$; $V^3|_b = 0$; $\frac{\partial\psi}{\partial\tau^0}\Big|_b = 0$; $\frac{\partial\psi}{\partial h^0}\Big|_b = 0$. The continuity condition is then satisfied identically.

As a result, we obtain a system of differential equations (9)-(11) for the following unknowns: the stream function, three contravariant components of the velocity vector V^3, and the contravariant component ω^3 of the vorticity.

In the given case, $\partial P/\partial q^3 = \text{const}$ can be found from Eq. (11),

$$\frac{\partial P}{\partial q^3} = \frac{1}{Q}\iint_\Omega \left\{ \frac{1}{q^1}\frac{\partial}{\partial q^1}\left[q^1\varphi_1 \left(A\frac{\partial V^3}{\partial q^1} - kq^1\frac{\partial}{\partial q^1}\left(\frac{1}{q^1}\cdot\frac{\partial\psi}{\partial q^1}\right)\right)\right] + \right.$$
$$\left. + \frac{\partial}{\partial q^2}\left[\varphi_1\left(\frac{A^2}{(q^1)^2}\frac{\partial V^3}{\partial q^2} - \frac{Ak}{q^1}\frac{\partial^2\psi}{\partial q^1\partial q^2} + \frac{2k}{(q^1)^2}\frac{\partial\psi}{\partial q^2}\right]\right\} d\Omega.$$

Algorithm for Solving the Problem and Results of Calculations. The method of finite elements was used to solve the systems of hydrodynamic equations in both the Galerkin approximation and the vorticity–stream function approximation. Algorithms for solving the stated problem were constructed on the iteration principle, including iterations to refine the approximate values of the components V^1 and V^2 of the velocity vector (internal iterations) and $\partial P/\partial q^3$ (external iterations).

For both methods we considered the case of a model fluid with parameters $\varphi_{1\Omega} = 0.9$ (Pa·sec) and $\varphi_{20} = 0.01$ (Pa·sec^2). The pipe diameter was D = 0.014 m and d/D = 0.720. The pitch S/D of the helical knurling was varied in the range 0.72-2.86.

In Figs. 1-3 we show the results of a calculation of the components of the velocity vector in dimensionless form for radial and annular cross sections of a channel (Fig. 1) with helical knurling. For convenience in presenting and analyzing the results, the distributions obtained for the components of the velocity vector were transformed to the cylindrical coordinate system using Eqs. (4) and (5).

As seen from Fig. 1, the curve of the axial component V_z of the velocity vector has a parabolic shape, and has a more bulging character in the vicinity of a rib of the helical knurling. A direct relationship is noted between the maximum value of V_z and the geometrical dimensions of the channel. For example, the largest value $(V_z)_{max}$ is reached for the largest ratio S/D = 2.86. The asymmetric distribution of the calculated curve of the component V_z relative to the axis of the helical channel (Fig. 1a) is explained by an increase in shear stress in the vicinity of a knurling rib and indicates the manifestation of viscoelastic properties.

An annular cross section (Fig. 1b) is also characterized by a parabolic distribution of V_z. Some asymmetry of the curve relative to the radial channel cross section A–A (Fig. 1a) may be ascribed to nonuniformity of the distribution of shear stress ahead of a rib of the helical knurling and behind it.

The radial component V_r of the velocity vector has its greatest influence in the wall region of flow. It decreases toward the center and V_r becomes negative.

The nature of the distribution of the calculated component V_r in the channel cross sections under consideration enables us to conclude that forces repelling the flow from the channel walls toward the center develop in the wall regions. The point at which V_r reaches a maximum is also found to depend directly on the geometrical characteristics of the channel. As seen from Fig. 2, with a decrease in the pitch of the helical knurling, the maximum of V_r shifts toward the center of the channel (dashed lines) and its absolute value increases.

A similar dependence can be noted for the component V_φ of the velocity vector (Fig. 3). Here the maximum of V_φ also shifts toward the center with a decrease in the pitch of the helical knurling (dashed lines).

The calculated distributions of the components V_r and V_φ in the annular cross section of the channel contain bends in the region adjacent to the rib of the helical knurling. This may be explained by the manifestation of nonlinear viscoelastic properties of the fluid and indicates a sharp increase in shear stress in the immediate vicinity of the rib.

These calculated distributions of the components V_r, V_φ, and V_z enable us to conclude that mixing of fluid layers occurs in the wall region of flow, the intensity of which depends directly on the geometrical characteristics of the channel.

To describe the influence of the rheological properties of the fluid on the hydrodynamic characteristics of the flow, we made calculations for media with the same parameter φ_{10}. In Fig. 4 we give curves of the dimensionless components V_z (Fig. 4a) and V_r (Fig. 4b) of the velocity vector for a non-Newtonian, a pseudoplastic, and a nonlinear viscoelastic fluid. As seen from Fig. 4, nonlinear viscoelasticity causes a more even distribution of V_z over the channel cross section. The maxima of the V_r curve are shifted most toward the channel wall in this case, and their absolute values are higher than for the Newtonian and pseudoplastic media. The V_z and V_r curves for a pseudoplastic fluid occupy an intermediate position between those for a Newtonian and a nonlinear viscoelastic fluid.

The curves of the components of the velocity vector obtained by solving the stated problem in the Galerkin approximation and in the vorticity–stream function form are almost identical. But it must be noted that the solution of the problem in the vorticity–stream function form is distinguished by being more cumbersome and less stable in the course of the calculations, which is explained by the more complicated nonlinear form of the free term in the system of differential equations (7)-(11). For example, two or three iterations were needed to provide a relative error $\varepsilon = 10^{-3}$ in the external block (calculation of $\partial P/\partial q^3$) when solving the problem in the Galerkin approximation, whereas five to seven iterations were needed to solve it by the variation method. About the same relationships were noted in calculations for the internal block (calculation of V^1 and V^2 in the Galerkin approximation and of ψ and ω^3 in the solution by the variation method). The cost in computer time to solve the problem increased accordingly.

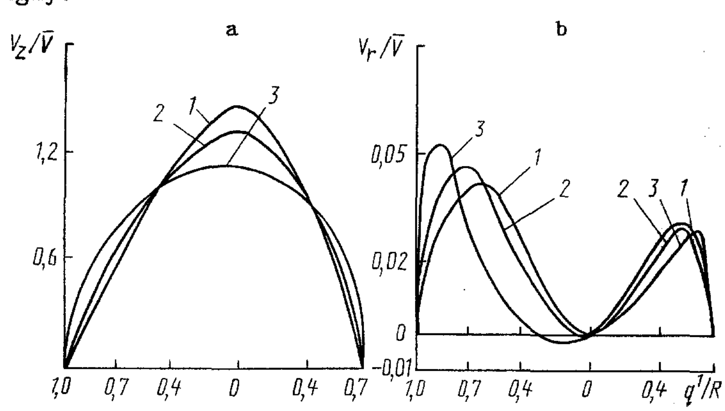

Fig. 4. Influence of the rheological properties of the fluid on the hydrodynamic characteristics of flow: a) axial component of the velocity vector in cross section A–A; b) radial component of the velocity vector in cross section A–A; 1) Newtonian fluid; 2) pseudoplastic fluid; 3) nonlinear viscoelastic fluid.

APPENDIX

The components of the deviator of the stress tensor T^0 are

$$T^0_{11} = 2\varphi_1 \frac{\partial}{\partial q^1}\left(\frac{1}{q^1}\frac{\partial\psi}{\partial q^2}\right);$$

$$T^0_{12} = T^0_{21} = \varphi_1\left(2\omega^3 q^1 - 2q^1\left(kV^3 - \frac{1}{q^1}\frac{\partial\psi}{\partial q^1}\right) + \frac{2}{q^1}\frac{\partial^2\psi}{(\partial q^2)^2}\right);$$

$$T^0_{13} = T^0_{31} = \varphi_1\left(2\omega^3 kq^1 - 2kq^1\left(kV^3 - \frac{1}{q^1}\frac{\partial\psi}{\partial q^1}\right) + k\frac{\partial^2\psi}{(\partial q^2)^2} + \frac{\partial V^3}{\partial q^1}\right);$$

$$T^0_{22} = 2(q^1)^2\varphi_1\frac{\partial}{\partial q^2}\left(kV^3 - \frac{1}{q^1}\frac{\partial\psi}{\partial q^1}\right) + 2\varphi_1\frac{\partial\psi}{\partial q^2} +$$

$$+ 2k^2(q^1)^4\varphi_2\left(\frac{\partial V^3}{\partial q^1}\right)^2 + A(2-A)\varphi_2\left(\frac{\partial V^3}{\partial q^2}\right)^2;$$

$$T^0_{23} = T^0_{32} = \varphi_1\left[A\frac{\partial V^3}{\partial q^2} - kq^1\frac{\partial^2\psi}{\partial q^1\partial q^2} + 2k\frac{\partial\psi}{\partial q^2}\right] - 2\varphi_2 Ak\left((q^1)^2\left(\frac{\partial V^3}{\partial q^1}\right)^2 + A\left(\frac{\partial V^3}{\partial q^2}\right)^2\right);$$

$$T^0_{33} = 2k^2q^1\varphi_1 V^1 - 2A^2\varphi_2\left[\left(\frac{\partial V^3}{\partial q^1}\right)^2 - \frac{2A}{(q^1)^2}\left(\frac{\partial V^3}{\partial q^2}\right)^2\right].$$

NOTATION

$A = 1 + (kq^1)^2$; B_N, Nth-order White–Metzner kinematic tensor; D, deformation-rate tensor; H^1_2, space of solenoidal vector functions; $\bar{h}$, element of the space H^1_2; I_2, I_3, second and third invariants of the deformation-rate tensor; I, identity tensor; $k = 2\pi/S$; L_0, L_1, L_2, linear operators; L, volume of space included between channel cross sections; n^0, normal to the channel contour; P, pressure; (q^1, q^2, q^3), helical coordinate system; Q, flow rate; (r, φ, z) cylindrical coordinate system; S, pitch of helical knurling; T^0, deviator of the stress tensor; $\bar{V}$, velocity vector; $\nabla\bar{V}$, velocity gradient tensor; $\nabla\bar{V}^t$, transposed tensor $\nabla\bar{V}$; V^1, V^2, V^3, components of $\bar{V}$ in the helical coordinate system; V_r, V_φ, V_z, components of $\bar{V}$ in the cylindrical coordinate system; ρ, density; σ, total stress tensor; τ^0, tangent to the channel contour; φ_1, φ_2, material functions of I_2; φ_{10}, φ_{20}, values of φ_1 and φ_2 as $I_2 \to 0$; ψ, stream function; Ω, region of transverse channel cross section; ω^2, third contravariant component of the vorticity vector. Indices: b, boundary of Ω.

LITERATURE CITED

1. S. B. Uttarwar and M. Raja Rao, Trans. ASME, J. Heat transfer, 107, No. 4, 930-935 (1985).
2. E. K. Kalinin, G. A. Dreitser, and S. A. Yarkho, Intensification of Heat Transfer in Channels [in Russian], Moscow (1990).
3. W. J. Marner and A. E. Bergles, "Augmentation of highly viscous laminar tubeside heat transfer by means of twisted tape insert and an internally finned tube," ASME National Heat Transfer Conference, Denver, 43, 19-28 (1985).
4. G. Astarita and G. Marrucci, Principles of Non-Newtonian Fluid Mechanics, McGraw-Hill, London–New York (1974).
5. Yu. G. Nazmeev, N. F. Zobin, and E. K. Vachagina, Inzh.-Fiz. Zh., 50, No. 6, 1034-1035 (1986).
6. Yu. G. Nazmeev, Inzh.-Fiz. Zh., 61, No. 2, 277-283 (1991).
7. V. G. Litvinov, Motion of a Nonlinearly Viscous Fluid [in Russian], Moscow (1982).